Aust. J. Phys., 1986, 39, 433–48

Scattering of Pulsar Radiation and Electron Density Turbulence in the Interstellar Medium

S. K. Alurkar,[A] O. B. Slee[B] and A. D. Bobra[A]

[A] Physical Research Laboratory, Ahmedabad 380009, India.
[B] Division of Radiophysics, CSIRO, P.O. Box 76, Epping, N.S.W. 2121.

Abstract

We report measurements, using the Culgoora circular array at 80 and 160 MHz and the Parkes 64 m telescope at 410 MHz, of the pulse broadening due to interstellar scattering on 33 pulsars. These results are added to published data on 52 other pulsars in order to investigate the interstellar turbulence levels over 85 paths in the Galaxy. We find a significant relation between the turbulence level C_n^2 and dispersion measure, heliocentric distance, galactocentric distance, galactic latitude and galactic longitude. Our results are consistent with a distribution of turbulence that peaks near the galactic centre and extends out to past the solar circle, with the scale height perpendicular to the plane at least equal to that of the pulsars. The magnitude of the fluctuations in electron density responsible for the scattering is not proportional to the average electron density, but increases much more rapidly than the latter as the galactic centre is approached. The apparent dependence of C_n^2 on heliocentric distance is preferentially interpreted as due to the presence of a highly clumped distribution of turbulence along all lines of sight.

1. Introduction

The amplitude scintillation of pulsar signals and the temporal broadening of their pulse profiles are different manifestations of scattering by fine-scale electron density fluctuations in the interstellar medium. Considerable evidence has now been obtained that the turbulence conforms to a power-law wavenumber spectrum of the form

$$P_{\delta N_e}(q) = C_n^2\, q^{-\alpha}, \qquad q_0 \leqslant q \leqslant q_1, \tag{1}$$

where q_0 and q_1 are wavenumber cutoffs and C_n^2 is the level of turbulence.

The observable quantities $\tau(\nu)$ and $\Delta\nu(\nu)$, which are respectively the $\exp(-1)$ width of the impulse scattering function and the decorrelation bandwidth of the amplitude scintillations, can be used to measure the strength of scattering along a line of sight to the pulsar. Both $\tau(\nu)$ and $\Delta\nu(\nu)$ vary in opposite senses as approximately the fourth power of the observing frequency, and the quantities are related by an equation of the form

$$2\pi K \Delta\nu\tau = 1, \tag{2}$$

where K depends on the turbulence spectrum and the distribution of turbulence but is typically of order unity. At low frequencies and/or large pulsar distances $\Delta\nu$ is only a few Hz and is thus not measurable with practicable radiometers; measurements of

0004-9506/86/030433$02.00

the pulse broadening τ then become a good means of determining C_n^2. On the other hand, at high frequencies and/or short pulsar distances τ becomes immeasurably small, but then it is possible to determine $\Delta\nu$, which may be as high as 1 or 2 MHz. In a small range of intermediate frequencies it is sometimes possible to measure both τ and $\Delta\nu$, and such measurements have been used to establish the validity of equation (2) (Slee *et al.* 1980).

The present paper presents the measurements, with the Culgoora circular array at 80 and 160 MHz, of pulse broadening τ on 16 pulsars; some of these observations were provisionally reported by Slee *et al.* (1980) but the present more thorough and systematic analysis of the data now supersedes the earlier results. We also include 410 MHz measurements of τ, made with the 64 m reflector at Parkes, for 17 highly scattered pulsars. We then supplement our measurements with determinations of either $\Delta\nu$ or τ from the literature for 52 additional pulsars and compute C_n^2 along 85 path-lengths in the Galaxy.

Section 2 provides a brief description of the observations at Culgoora and Parkes used to provide the new or revised determinations of pulse broadening. Section 3 presents the new results (Table 1), tabulates the results that have been collected from the literature (Table 2) and then combines all measurements to produce 85 estimates of delay time at 0·30 GHz and the resulting computed values of C_n^2 (Table 3). Section 4 examines the dependence of C_n^2 on dispersion measure, distance and galactic coordinates. Our conclusions are offered in Section 5.

2. Observations

The Culgoora observations at 80 and 160 MHz were made during the interval from April 1979 to November 1980 and included 14 observing sessions each of about five days duration. The equipment, observing technique and method of profile analysis have been described in detail by Slee *et al.* (1980); the observational data are identical with those used in a companion paper dealing with the pulsar fluxes (Slee *et al.* 1986). A total of 43 pulsars were detected out of a total of 74 observed pulsars, but unambiguous pulse widening due to interstellar scattering was present in only 16 pulsars.

Briefly, a typical Culgoora observation consisted of tracking the pulsar for ~ 1 h with the central declination beam of the circular array, sometimes alternating the observing frequency between 160 and 80 MHz on successive 60 s intervals. The pulses were de-dispersed by applying the i.f. signal simultaneously to two filter banks, one consisting of 9×90 kHz bandwidth filters, the other 15×10 kHz bandwidth filters. The outputs of the filters were sampled at 3·9 ms intervals and summed with appropriate digital delays to compensate for the differential time delays introduced by the interstellar electron density. The two de-dispersed outputs were averaged for intervals of 60 s by stacking the data in 3·9 ms bins synchronously with the apparent pulse period; for each pulsar some 30 to 120 such integrations were later averaged off-line to produce the final profile. An attempt was made to observe each scattered profile during several observing sessions in order to improve the accuracy of our estimate of τ. If pulse broadening were seen at 160 MHz its $\sim\nu^{-4}$ dependence ensured that the pulse would generally not be detected at 80 MHz. In only one case (1749−28) was the scattering measurable at both frequencies.

The 410 MHz measurements were obtained during observations of pulsar timing in 11 sessions with the Parkes 64 m telescope in 1978 and 1979 (Newton *et al.*

1981). The receiver consisted of a dual-channel system receiving orthogonal linear polarizations at 410 MHz. Each of the two i.f. channels was split into 24 adjacent frequency bands, each of width 250 kHz, and the detected outputs of corresponding filters were summed and sampled at 5 ms intervals. The data were de-dispersed and folded at the apparent period and the integrated profile was written on magnetic tape. The integration time per profile was between 6 and 20 min, depending on the flux density of the pulsar. A total of 124 southern pulsars were observed during this program; 17 profiles showing clear exponential tails indicative of pronounced scattering have been included in this paper.

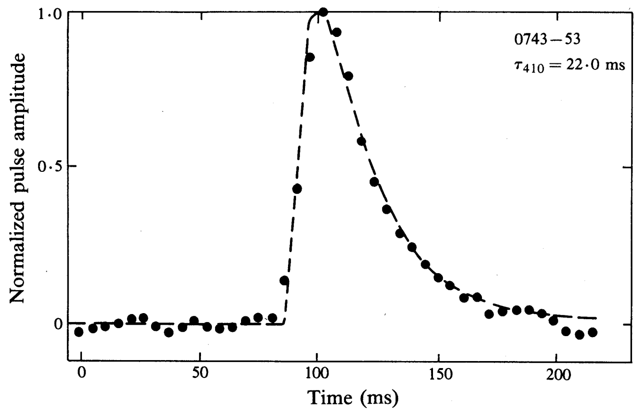

Fig. 1. Averaged profile of PSR 0743 − 53 taken with the Parkes 64 m telescope at 410 MHz. Circles represent the observed data sampled at 5 ms intervals. The dashed curve is the least-squares-fitted theoretical profile described in the text.

A theoretical scattered pulse profile was generated by successively convolving a gaussian profile representing the intrinsic pulse with: (i) an impulse scattering function of the form $\exp(-t/\tau)$; (ii) a gaussian function representing the effects of interstellar dispersion across the filter bandpass; (iii) an exponential function representing the post-detector RC time constant. This theoretical profile was least-squares-fitted to the observed profile, with τ as the adjustable parameter. The width of the intrinsic profile for the 80 and 160 MHz observations was taken as the width listed by Manchester and Taylor (1981) from measurements at frequencies of 408 MHz or higher. The intrinsic widths for the 410 MHz scattered profiles were assumed to be 3·0% of the pulse period, since no higher-frequency measurements were available; however, in all cases the deduced pulse broadening is a significant fraction of the pulse period, so that inaccuracies in the assumed width should not be important. We show an example of a fitted profile in Fig. 1.

3. Results

The new and revised measurements of pulse widening from Culgoora observations at 80 and 160 MHz and Parkes observations at 410 MHz are presented in Table 1. The Culgoora results replace and extend those published by Slee *et al.* (1980). The value of τ comes from the best-fitting truncated exponential scattering function $\exp(-t/\tau)$. The standard errors for τ were computed as follows: (i) if there are >3 independent measurements the standard error is that of the mean; (ii) if there are $\leqslant 3$ measurements (as for all the 410 MHz results) we have compared the quality of the fit (as defined by the r.m.s. scatter) with the quality of fits obtained on well-observed pulsars for which the standard errors are available.

Table 1. Culgoora and Parkes measurements of pulse widening

Pulsar	DM[A] (cm^{-3} pc)	ν (GHz)	No. of obs.	τ (ms)	Std error in τ (ms)
0450−18	39·9	0·16	7	5·8	1·6
0740−28	73·8	0·16	9	24·5	2·8
0743−53	122·3	0·41	1	22·0	2·6
0808−47	228·3	0·41	1	33·0	1·5
0833−45	69·1	0·16	6	621	109
0835−41	147·6	0·16	7	24·0	5·5
0839−53	155·6	0·41	1	20·0	2·4
1015−56	439·1	0·41	1	6·0	0·4
1030−58	418·9	0·41	1	45·0	6·3
1054−62	323·4	0·41	1	23·0	2·5
1114−41	41·4	0·16	4	7·4	2·9
1154−62	325·2	0·41	1	27·0	1·7
1302−64	505·8	0·41	1	25·0	2·1
1323−63	505·3	0·41	1	31·0	2·8
1323−62	318·4	0·41	1	185	35
1323−58	283·2	0·41	1	77·0	15
1356−60	295·0	0·41	1	24·0	1·7
1558−50	169·5	0·41	1	20·8	2·2
1620−42	295·2	0·41	1	36·0	4·7
1737−39	158·5	0·41	1	11·0	0·8
1749−28	50·9	0·16	3	2·9	0·1
		0·08	5	24·9	2·0
1818−04	84·4	0·16	10	50·3	5·0
1821−19	225·7	0·41	1	17·0	1·3
1844−04	141·9	0·16	1	63·5	30
1907+02	168	0·16	2	27·9	16
1907+10	144	0·16	3	26·5	8·1
1911−04	89·4	0·16	8	16·7	1·8
1915+13	94	0·16	7	11·7	1·9
1920+21	220	0·16	2	96·8	50
1933+16	158·5	0·16	6	21·7	1·6
1940−12	29·1	0·16	3	4·4	1·1
2123−67	34·7	0·41	1	8·0	0·9
2303+30	49·9	0·16	3	9·9	3·6

[A] Values of dispersion measure DM from Manchester and Taylor (1981).

Table 2 lists measurements from the literature of τ and $\Delta\nu$ for 59 pulsars, some of which also contribute data to Table 1. We do not include the errors, but in many cases these may be obtained from the original references.

Table 3 summarizes the measurements on all 88 pulsars in Tables 1 and 2. In order to systematically compute the turbulence levels C_n^2 we have transformed all measurements of $\tau(\nu)$ and $\Delta\nu(\nu)$ to $\tau_{0\cdot 30}$ (the pulse widening at 0·30 GHz); we have chosen a standard frequency of 0·30 GHz because the observing frequencies are clustered around 160, 320 and 408 MHz and the scaling error will be minimized if

Table 2. Additional measurements from the literature

Pulsar	DM[A] (cm^{-3} pc)	ν (GHz)	Measurement type	Value[B] (ms, kHz)	Ref.[C]	Pulsar	DM[A] (cm^{-3} pc)	ν (GHz)	Measurement type	Value[B] (ms, kHz)	Ref.[C]
0301+19	15·7	0·43	$\Delta\nu$	83	1	1749−28	50·9	0·33	$\Delta\nu$	6·0	4
0329+54	26·8	0·41	$\Delta\nu$	100	2			0·41	$\Delta\nu$	7·0	4
0355+54	57·0	1·41	$\Delta\nu$	575	3			0·63	$\Delta\nu$	93	4
0525+21	50·9	0·43	$\Delta\nu$	50	1	1758−23	1140	1·4	τ	130	7
0540+23	77·6	0·43	$\Delta\nu$	1·9	1	1821+05	67·5	0·43	$\Delta\nu$	19	1
0611+22	96·7	0·43	$\Delta\nu$	0·72	1	1839+09	48·7	0·43	$\Delta\nu$	8·2	1
0626+24	82·9	0·43	$\Delta\nu$	3·5	1	1842+14	39	0·43	$\Delta\nu$	33	1
0628−28	34·4	0·33	$\Delta\nu$	265	4	1845−01	163	0·43	τ	42·0	5
		0·41	$\Delta\nu$	340	4	1859+03	402·9	0·32	τ	187	2
		0·63	$\Delta\nu$	1600	4			0·43	τ	65·0	5
0656+14	14	0·43	$\Delta\nu$	144	1	1900+01	243·4	0·43	τ	11·0	5
0820+02	22·2	0·43	$\Delta\nu$	178	1	1907+02	168	0·32	τ	3·0	1
0823+26	19·5	0·04	τ	20·0	2	1907+10	144	0·32	τ	2·2	1
		0·43	$\Delta\nu$	305	1	1913+10	240	0·43	τ	14·6	6
0834+06	12·9	0·43	$\Delta\nu$	229	1	1914+13	230	0·32	τ	5·5	1
0833−45	69·1	0·30	τ	9·4	2	1919+20	70	0·43	τ	11·7	5
0919+06	27·2	0·43	$\Delta\nu$	46	1	1919+21	12·4	0·32	$\Delta\nu$	25	1
0943+10	15·4	0·43	$\Delta\nu$	903	1			0·43	$\Delta\nu$	158	1
0950+08	3·0	0·32	$\Delta\nu$	990	1	1929+10	3·2	0·32	$\Delta\nu$	859	1
		0·43	$\Delta\nu$	1089	1	1929+20	210	0·43	τ	4·83	6
1133+16	4·8	0·43	$\Delta\nu$	917	1	1933+16	158·5	0·11	τ	67·0	2
1237+25	9·3	0·43	$\Delta\nu$	767	1			1·415	$\Delta\nu$	112	2
1323−62	318·4	0·75	τ	30·0	2			1·67	$\Delta\nu$	110	4
1451−68	8·6	0·33	$\Delta\nu$	260	4	1933+17	210	0·43	τ	15·0	1
		0·41	$\Delta\nu$	580	4	1933+15	165	0·43	τ	5·8	6
		0·63	$\Delta\nu$	2000	4	1943+18	215	0·43	τ	15·0	1
1530+27	13·6	0·43	$\Delta\nu$	515	1	1944+17	16·3	0·43	$\Delta\nu$	72	1
1541+09	35·0	0·43	$\Delta\nu$	5·7	1	1946+35	129·1	0·32	τ	32·0	2
1557−50	270	0·75	τ	16·0	2			0·43	τ	15·0	5
1604−00	10·7	0·32	$\Delta\nu$	312	1	1952+29	7·9	0·43	$\Delta\nu$	1170	1
		0·43	$\Delta\nu$	1089	1	2002+31	233	0·32	τ	10·0	2
1612+07	22·0	0·43	$\Delta\nu$	345	1	2016+28	14·2	0·43	$\Delta\nu$	123	1
1641−45	475	0·75	τ	40·0	2	2020+28	24·6	0·43	$\Delta\nu$	159	1
1642−03	35·7	0·33	$\Delta\nu$	20	4	2044+15	38·8	0·43	$\Delta\nu$	9·0	1
		0·41	$\Delta\nu$	42	4	2053+36	97·1	0·32	τ	7·7	1
		0·63	$\Delta\nu$	670	4			0·43	τ	2·7	1
1737+13	48·4	0·43	$\Delta\nu$	36	1	2303+30	49·9	0·43	$\Delta\nu$	2·2	1
						2315+21	19·4	0·43	$\Delta\nu$	315	1
						2319+60	96·0	1·41	$\Delta\nu$	175	3

[A] Values of DM from Manchester and Taylor (1981).
[B] Multiple measurements at the same frequency have been averaged.
[C] References: 1, Cordes *et al.* (1985); 2, Rickett (1977); 3, Wolszczan *et al.* (1974); 4, Roberts and Ables (1982); 5, Rankin and Benson (1981); 6, Gullahorn and Rankin (1978); 7, Manchester *et al.* (1985).

Table 3. Levels of turbulence along directions to pulsars

Pulsar	DM (cm^{-3} pc)	No. freq. averaged	$\tau_{0\cdot 3}$ (ms)	log C_n^2 ($m^{-20/3}$)	Distance L (kpc)	Distance R (kpc)	Galactic coords l (deg.)	Galactic coords b (deg.)
0301+19	15·7	1	0·0095	−2·67	0·56	10·4	161·1	−33·3
0329+54	26·8	1	0·0064	−3·94	2·3	12·0	145·0	−1·2
0355+54	57·0	1	0·27	−2·30	1·6	11·3	148·2	+0·8
0450−18	39·9	1	0·35	−2·20	1·6	11·1	217·1	−34·1
0525+21	50·9	1	0·016	−3·51	2·0	12·0	183·9	−6·9
0540+23	77·6	1	0·42	−2·53	2·6	12·6	184·4	−3·3
0611+22	96·7	1	1·1	−2·37	3·3	13·3	188·9	+2·4
0626+24	82·9	1	0·23	−2·92	3·2	13·1	188·8	+6·2
0628−28	34·4	3	0·0015	−4·01	1·3	10·7	237·0	−16·8
0656+14	14	1	0·0055	−2·61	0·40	10·4	201·2	+8·2
0740−28	73·8	1	1·5	−1·63	1·5	10·7	243·8	−2·4
0743−53	122·3	1	88	−0·53	2·4	10·4	266·6	−14·3
0808−47	228·3	1	132	−1·07	5·7	12·0	263·3	−8·0
0820+02	22·2	1	0·0044	−3·22	0·79	10·6	222·0	+21·2
0823+26	19·5	2	0·0026	−3·33	0·71	10·6	197·0	+31·7
0833−45	69·1	2	24	+0·24	0·50	10·1	263·6	−2·8
0834+06	12·9	1	0·0035	−2·83	0·43	10·3	219·7	+26·3
0835−41	147·6	1	1·5	−2·01	2·4	10·7	260·9	−0·3
0839−53	155·6	1	80	−0·76	3·1	10·4	270·8	−7·1
0919+06	27·2	1	0·017	−2·92	1·0	10·6	225·4	+36·4
0943+10	15·4	1	0·00087	−3·54	0·56	10·3	225·4	+43·1
0950+08	3·0	2	0·00033	−2·43	0·09	10·0	228·9	+43·7
1015−56	439·1	1	24	−2·40	14·0	15·1	282·7	+0·3
1030−58	418·9	1	181	−1·73	15·0	15·9	285·9	−1·0
1054−62	323·4	1	92	−1·24	6·0	9·7	290·3	−3·0
1114−41	41·4	1	0·45	−2·06	1·5	9·7	284·5	+18·1
1133+16	4·8	1	0·00086	−2·49	0·15	10·0	241·9	+69·2
1154−62	325·2	1	108	−1·30	7·0	9·3	296·7	−0·2
1237+25	9·3	1	0·0010	−3·06	0·33	10·0	252·5	+86·5
1302−64	505·8	1	100	−2·13	19·0	15·9	304·4	−2·1
1323−63	505·3	1	124	−2·01	18·0	14·7	306·7	−1·5
1323−62	318·4	2	1260	−0·51	7·9	8·2	307·1	+0·2
1323−58	283·2	1	309	−1·19	9·8	8·8	307·5	+3·6
1356−60	295·0	1	96	−1·53	8·8	7·8	311·2	+1·1
1451−68	8·6	3	0·0012	−2·71	0·23	9·8	313·9	−8·5
1530+27	13·6	1	0·0015	−3·23	0·49	9·8	43·5	+54·5
1541+09	35·0	1	0·14	−2·38	1·3	9·1	17·8	+45·8
1557−50	270	1	944	−0·61	7·8	5·0	330·7	+1·6
1558−50	169·5	1	83	−0·58	2·5	7·9	330·7	+1·3
1604−00	10·7	2	0·00070	−3·27	0·36	9·7	10·7	+35·5
1612+07	22·0	1	0·0023	−3·47	0·80	9·4	20·6	+38·2
1620−42	295·2	1	144	−1·40	9·0	3·6	338·9	+4·6
1641−45	475	1	2360	+0·03	5·3	5·4	339·2	−0·2
1642−03	35·7	3	0·0099	−3·33	1·3	8·9	14·1	+26·1
1737−39	158·5	1	44	−1·38	5·1	5·1	350·6	−4·7
1737+13	48·4	1	0·022	−3·30	1·8	8·8	37·1	+21·7
1749−28	50·9	5	0·085	−2·35	1·0	9·0	1·5	−1·0
1758−23	1140	1	123000	+0·96	10·0	1·2	6·8	−0·1
1818−04	84·4	1	3·1	−1·37	1·5	8·7	25·5	+4·7
1821−19	225·7	1	68	−1·45	6·8	3·7	12·3	−3·1
1821+05	67·5	1	0·042	−3·27	2·3	8·2	35·0	+8·9

Table 3. *(Continued)*

Pulsar	DM (cm^{-3} pc)	No. freq. averaged	$\tau_{0\cdot3}$ (ms)	log C_n^2 ($m^{-20/3}$)	Distance L (kpc)	R (kpc)	Galactic coords l (deg.)	b (deg.)
1839+09	48·7	1	0·096	−2·62	1·5	8·9	40·1	+6·3
1842+14	39	1	0·024	−3·01	1·3	9·2	45·6	+8·1
1844−04	141·9	1	3·9	−2·00	3·7	7·0	28·9	−0·9
1845−01	163	1	208	−0·58	3·8	7·1	31·3	0·0
1859+03	402·9	2	286	−1·31	11·0	6·7	37·2	−0·6
1900+01	243·4	1	55	−1·28	5·0	6·6	35·7	−2·0
1907+02	168	2	2·9	−2·40	5·3	6·7	37·6	−2·7
1907+10	144	2	2·3	−2·24	3·9	7·7	44·8	+1·0
1911−04	89·4	1	1·0	−2·32	3·0	7·6	31·3	−7·1
1913+10	240	1	72	−1·38	6·4	7·1	44·7	−0·7
1914+13	230	1	7·3	−2·14	5·9	7·4	47·6	+0·5
1915+13	94	1	0·71	−2·27	2·4	8·6	48·3	+0·6
1919+20	70	1	58	−0·57	2·1	9·0	54·2	+2·6
1919+21	12·4	2	0·0063	−2·40	0·33	9·8	55·8	+3·5
1920+21	220	1	5·9	−2·40	7·4	8·4	55·3	+2·9
1929+10	3·2	1	0·00025	−2·45	0·08	9·9	47·4	−3·9
1929+20	210	1	24	−1·69	5·7	8·2	55·6	+0·6
1933+15	165	1	29	−1·56	5·3	7·9	51·9	−2·5
1933+16	158·5	4	1·6	−2·70	6·0	7·9	52·4	−2·1
1933+17	210	1	74	−1·36	6·3	8·1	53·7	−1·3
1940−12	29·1	1	0·27	−1·92	1·0	9·2	27·3	−17·2
1943+18	215	1	74	−1·47	7·3	8·4	55·6	−3·0
1944+17	16·3	1	0·011	−2·41	0·43	9·8	55·3	−3·5
1946+35	129·1	2	58	−1·19	4·6	9·5	70·7	+5·0
1952+29	7·9	1	0·00068	−2·81	0·20	9·9	65·9	+0·8
2002+31	233	1	13	−2·17	8·0	10·3	69·0	0·0
2016+28	14·2	1	0·0064	−3·49	1·3	9·6	68·1	−4·0
2020+28	24·6	1	0·0050	−3·58	1·3	9·6	68·9	−4·7
2044+15	38·8	1	0·088	−2·60	1·4	9·4	61·1	−16·8
2053+36	97·1	2	12	−1·53	3·4	9·9	79·1	−5·6
2123−67	34·7	1	32	−0·40	1·3	9·2	326·4	−39·8
2303+30	49·9	2	0·48	−2·23	1·9	10·4	97·7	−26·7
2315+21	19·4	1	0·0025	−3·35	0·71	10·1	95·8	−36·1
2319+60	96·0	1	0·88	−2·32	2·8	11·4	112·1	−0·6

we scale to a frequency near the centre of the range. We have used the equation $2\pi\Delta\nu\tau = 1$ to transform from one type of measurement to the other at the same frequency. In order to scale the observed values to $\tau_{0\cdot30}$ we have used $\tau \propto \nu^{-4\cdot45}$, which is the average frequency dependence of $\tau(\nu)$ for several well-observed pulsars (see e.g. Table 4 of Cordes *et al.* 1985).

The computation of C_n^2 has been discussed by several authors. Here we use the treatment given by Cordes *et al.* (1985). At 0·30 GHz their equation (6), evaluated with provision for line of sight averaging and by assuming a Kolmogorov turbulence spectrum ($\alpha = 11/3$ in our equation 1), reduces to

$$C_n^2 = 2\cdot42(\Delta\nu)_{0\cdot30}^{-0\cdot833}\, L^{-1\cdot833}, \tag{3}$$

where $(\Delta\nu)_{0\cdot30}$ is the decorrelation bandwidth in Hz and L is the pulsar distance in kiloparsecs.

4. Distribution of Turbulence in the Galaxy

(a) $\tau_{0\cdot30}$ against Dispersion Measure (DM)

The most direct method of investigating the scattering along different lines of sight is to plot $\tau_{0\cdot30}$ of Table 3 against DM. Fig. 2 shows the result for 85 pulsars.

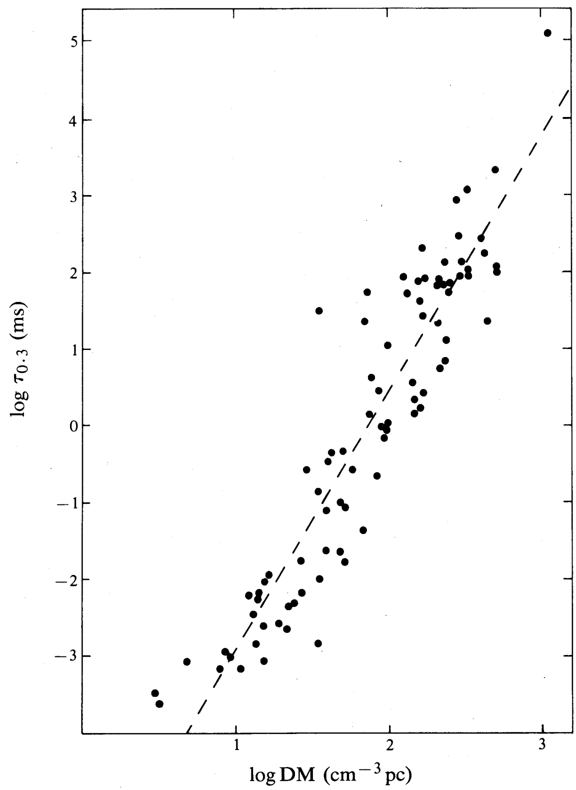

Fig. 2. Plot of collected measurements of the $0\cdot3$ GHz pulse broadening $\tau_{0\cdot3}$ against DM for the 85 pulsars listed in Table 3. The least-squares-fitted dashed line has a slope of $3\cdot32\pm0\cdot15$.

It is clear that despite considerable scatter there is a well-defined relation between $\tau_{0\cdot30}$ and DM. Least-squares fitting of power laws for various subsets of pulsars are summarized in Table 4; these show that the relation is a particularly constant one, with a high level of significance. The regression equation is not only independent of galactic coordinates but also of the ranges of DM making up the subsets; for example, the average DM of the pulsars in the $|b| < 5°$ subset is $3\cdot6$ times that of the $|b| \geqslant 5$ subset. The overall slope of $3\cdot32\pm0\cdot15$ is statistically indistinguishable from that deduced by Slee *et al.* (1980) from only 31 pulsars; hence the addition of more pulsars is unlikely to change its value significantly.

The expected slope for a Kolmogorov spectrum of turbulence which is uniformly distributed along the line of sight is $2\cdot2$. The observed, much steeper, slope is obviously connected with the fact that the turbulence is not uniform. Whether it is non-uniform in the sense of clumping or whether the non-uniformity arises because the spatial scales contributing to the scattering cannot be represented by a simple power law (see Cordes *et al.* 1985) is not clear. The question will be discussed further in Section 5.

Table 4. Least-squares fitted relationships

Fitted parameters	No. of pulsars	Fitted regression equation	Stand. error in slope	Coeff. of determination	Conf. level (%)
		$\tau_{0\cdot30}$ against dispersion measure			
All pulsars	85	$\tau_{0\cdot30} = 6\cdot21\times10^{-7}(\mathrm{DM})^{3\cdot32}$	0·15	0·858	>99·9
$\|b\| < 5°$	49	$\tau_{0\cdot30} = 1\cdot08\times10^{-6}(\mathrm{DM})^{3\cdot22}$	0·19	0·855	>99·9
$\|b\| \geqslant 5°$	36	$\tau_{0\cdot30} = 4\cdot84\times10^{-7}(\mathrm{DM})^{3\cdot36}$	0·35	0·725	>99·9
$\|l\| < 60°$	46	$\tau_{0\cdot30} = 5\cdot95\times10^{-7}(\mathrm{DM})^{3\cdot36}$	0·22	0·843	>99·9
$\|l\| > 60°$	39	$\tau_{0\cdot30} = 9\cdot00\times10^{-7}(\mathrm{DM})^{3\cdot18}$	0·22	0·851	>99·9
		C_n^2 against heliocentric distance[A]			
All pulsars	81	$\log C_n^2 = -2\cdot73+0\cdot20L$	0·03	0·303	>99·9
$\|b\| < 5°$	45	$\log C_n^2 = -2\cdot35+0\cdot14L$	0·04	0·182	99·0
$\|b\| \geqslant 5°$	36	$\log C_n^2 = -3\cdot14+0\cdot38L$	0·10	0·289	>99·9
$\|l\| < 60°$	44	$\log C_n^2 = -2\cdot58+0\cdot18L$	0·04	0·316	>99·9
$\|l\| > 60°$	37	$\log C_n^2 = -2\cdot85+0\cdot22L$	0·08	0·184	99·0
$\|l\| < 60°$, $\|b\| < 5°$	31	$\log C_n^2 = -2\cdot08+0\cdot11L$	0·05	0·162	98·0
		C_n^2 against galactocentric distance[A]			
All pulsars	81	$C_n^2 = 24\cdot90R^{-3\cdot71}$	0·70	0·262	>99·9
$\|b\| < 5°$	45	$C_n^2 = 14\cdot13R^{-3\cdot20}$	0·70	0·326	>99·9
$\|b\| \geqslant 5°$	36	Not significant			
$\|l\| < 60°$	44	$C_n^2 = 25\cdot20R^{-3\cdot72}$	0·79	0·348	>99·9
$\|l\| > 60°$	37	Not significant			
$\|l\| < 60°$, $\|b\| < 5°$	31	$C_n^2 = 8\cdot08R^{-2\cdot85}$	0·70	0·368	>99·9

[A] The four pulsars with $L \geqslant 14$ kpc in Fig. 3 have been omitted from the regressions.

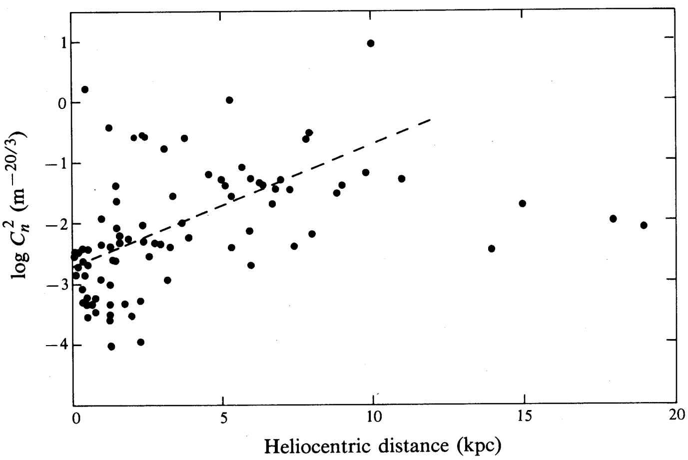

Fig. 3. Plot of the turbulence level C_n^2 against heliocentric distance. The least-squares-fitted dashed line (excluding the four values on the extreme right) corresponds to the exponential $\log C_n^2 = -2\cdot73+0\cdot20L$.

(b) C_n^2 against Heliocentric Distance (L)

The calculation of the turbulence coefficient C_n^2 is an attempt to remove the effects of varying path-lengths to various pulsars, making it possible to determine the average levels of turbulence in various directions. Fig. 3 is a plot of C_n^2 against heliocentric distance L for the 85 pulsars. It seems that C_n^2 increases with distance, as would be expected from the steeper-than-predicted increase of $\tau_{0\cdot30}$ with DM seen in Fig. 2.

The high scatter in Fig. 3 probably arises because of the uncertainty in the distance, which is used both as the abscissa and in computing C_n^2 from equation (3). Pulsar distances, which are computed from their dispersion measures with the help of a model for the galactic electron density distribution, may be in error by up to a factor of 2 (Lyne *et al.* 1985). For a Kolmogorov turbulence spectrum such an error introduces an error in log C_n^2 of $\pm 0{\cdot}52$.

The results of least-squares fitting of exponential regression equations for various subsets of pulsars are listed in Table 4. Power-law regressions were also tried, but in each subset the exponential equation accounted for significantly more of the variance. It should be noted that the four pulsars in our sample with the highest computed distances have only moderate values of C_n^2 (see Fig. 3). One explanation would be that these pulsars are seen through discrete HII regions, which would increase their dispersion measures (computed distances) much more than they would contribute to the scattering. Accepting this hypothesis, we have therefore omitted these pulsars from our regression analysis, although even if these data are admitted the relationships remain significant at only a slightly reduced confidence level.

It is clear from Table 4 that the apparent increase in C_n^2 with heliocentric distance is a general property of the subsets, with C_n^2 showing a similar trend both towards and away from the galactic centre. The 95% confidence intervals for the slopes of the regression equations do overlap, suggesting that there is no evidence for a change in the dependence of C_n^2 on distance when looking in various directions. Our best estimate for the magnitude of the effect comes from the regression equation for all pulsars.

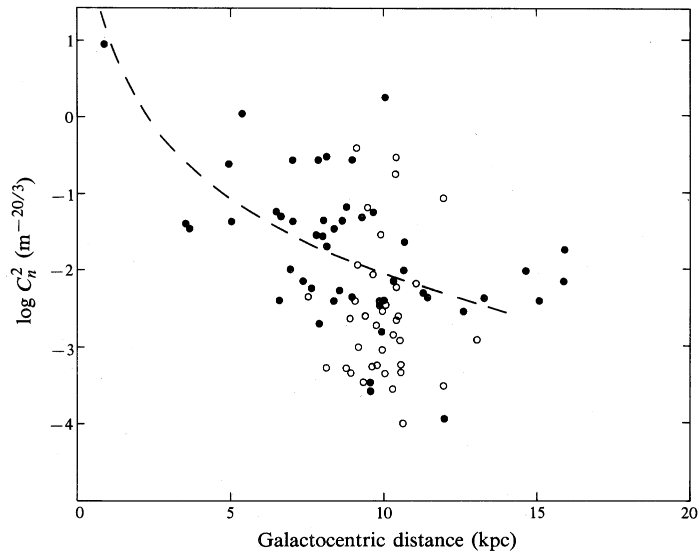

Fig. 4. Plot of the turbulence level C_n^2 against galactocentric distance. Closed circles refer to the pulsars with $|b| < 5°$, open circles to the pulsars with $|b| \geqslant 5°$. The dashed curve has been fitted to the closed circles (excluding the four values on the extreme right) and corresponds to the power law $C_n^2 = 14{\cdot}13R^{-3{\cdot}20}$.

(c) C_n^2 against Galactocentric Distance (R)

The turbulence coefficient C_n^2 is plotted against the pulsar galactocentric distance R in Fig. 4. Since both C_n^2 and R are derived by using the heliocentric distance,

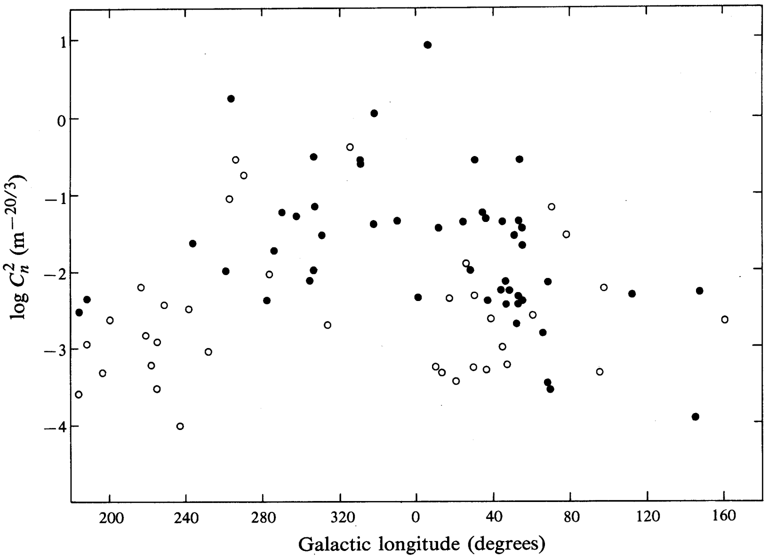

Fig. 5. Plot of the turbulence level against galactic longitude. Closed circles refer to the 49 pulsars with $|b| < 5°$, open circles to the 36 pulsars with $|b| \geqslant 5°$.

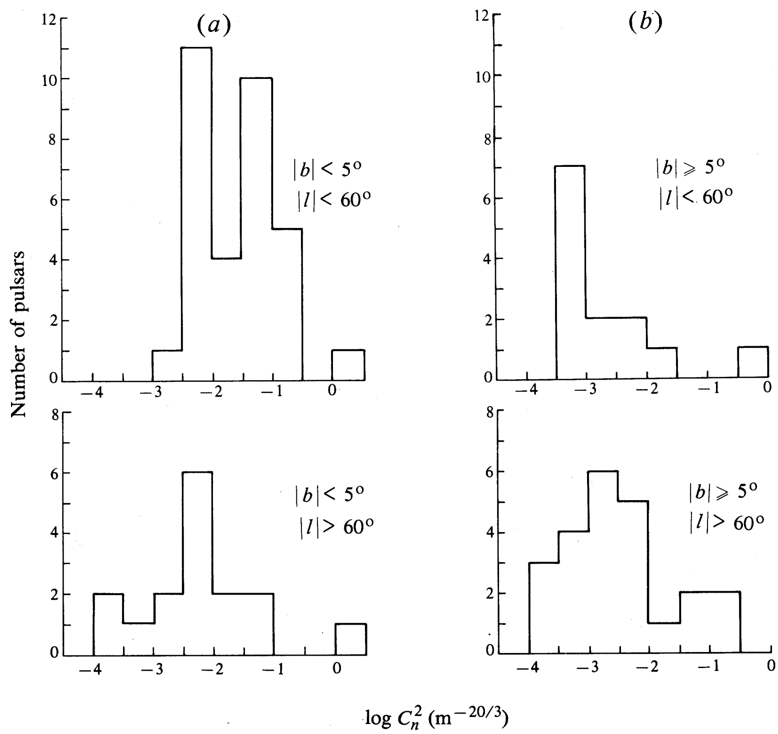

Fig. 6. Distributions of turbulence levels for (*a*) the low-latitude pulsars ($|b| < 5°$) and (*b*) the high-latitude pulsars ($|b| \geqslant 5°$) in directions towards the galactic centre ($|l| < 60°$) and away from the galactic centre ($|l| > 60°$).

which may be in error by up to a factor of 2, there would be considerable scatter in this diagram even if there were a tight relationship between the two quantities.

We have fitted power-law regression equations of C_n^2 on R for various combinations of galactic coordinates; the fitted parameters are given in Table 4. The inverse relationships between C_n^2 and R for these equations are formally significant at the 99·9% confidence level. It seems clear that the turbulence decreases steeply with galactocentric distance for the three groups of pulsars with significant regression equations. This behaviour is not confined to pulsars near the galactic plane—for example, the group with $|l| < 60°$ has a median distance perpendicular to the galactic plane of $\bar{z}_{\rm PSR} = 0 \cdot 17$ kpc yet its C_n^2/R dependence is as steep and as significant as the group with $|b| < 5°$, with a median $\bar{z}_{\rm PSR} = 0 \cdot 07$ kpc.

We note that the galactocentric dependence is much stronger than the apparent dependence on heliocentric distance; for example, for the group $|l| < 60°$, $|b| < 5°$, which encompasses directions with a predominant component towards the galactic centre, the increase in C_n^2 while traversing the range of galactocentric distance $1 < R < 10$ kpc (i.e. out to the Sun) is $\sim$700—however, the increase in C_n^2 due to the heliocentric distance (most accurately obtained from the relation for all pulsars in Table 4) is only 62. We do not believe that the weaker C_n^2/L dependence is merely a reflection of the much stronger C_n^2/R relation—our major reason for this statement is that the C_n^2/L dependence is very significant for those pulsars in directions well away from the galactic centre (e.g. the group in Table 4 with $|l| > 60°$) for which R is either constant or increasing as L increases.

(d) C_n^2 against Galactic Coordinates (l, b)

Fig. 5 is a plot of C_n^2 against galactic longitude; pulsars in the two ranges of latitude $|b| < 5°$ and $|b| \geqslant 5°$ are the closed and open circles respectively. For the low-latitude pulsars there appears to be an increase in C_n^2 within $\sim$60° either side of the galactic centre. More quantitatively, Fig. 6 shows the distributions of C_n^2 for (*a*) pulsars with $|b| < 5°$ and split into two longitude ranges $|l| < 60°$ and $|l| > 60°$, and (*b*) pulsars with $|b| \geqslant 5°$ and split into the same longitude ranges.

It is clear from Fig. 6*a* that for low-latitude pulsars C_n^2 increases by a factor of $\sim$6·5 as the line of sight comes within $\sim$60° of the galactic centre. This increase is not seen for the higher-latitude pulsars (Fig. 6*b*). The differences between the distributions of Figs 6*a* and 6*b* can be wholly explained by the differing galactocentric and heliocentric distances of the pulsars in them and the dependences of C_n^2 on these distances as described in the last two subsections. For example, for $|l| < 60°$ in Fig. 6*a* the shift in the distribution (significant at the 98% confidence level on a Kruskal–Wallis ranking test) towards larger C_n^2 is due to the fact that the median R for this sample is a factor of 1·35 smaller and its median L a factor of 2·3 greater than the corresponding medians for the lower distribution. The distributions in Fig. 6*b*, on the other hand, do not differ significantly, because their medians R differ by only 1·13 and their medians L are identical.

(e) C_n^2 against Distance from the Plane $|z|$

The parameters for the distributions of $|z| = L \sin |b|$ are given in Table 5. The quantity $\bar{z}_{\rm PSR}$ is the mean or median $|z|$ for a particular subset of pulsars. We prefer to use the median values in the following quantitative comparisons because of the presence of significant skewness in some of these distributions (e.g. the distribution $|b| < 5°$). The parameter

$$\bar{z}_{\delta N_e} = \sum_i C_{ni}^2 |z_i|_{\mathrm{PSR}} \Big/ \sum_i C_{ni}^2 \tag{4}$$

is a *weighted* average of $|z|$ with weights proportional to C_n^2 for each pulsar. It is thus a measure of the spread of the turbulence above and below the galactic plane. If the scale height for the turbulence is of the order of, or greater than, the scale height for the pulsars then C_{ni}^2 will not vary much with $|z_i|_{\mathrm{PSR}}$ and $\bar{z}_{\delta N_e} \sim \bar{z}_{\mathrm{PSR}}$. On the other hand, if the scale height for the turbulence is considerably less than that for the pulsars then the weighting in equation (4) will discriminate against the high $|z|$ pulsars and $\bar{z}_{\delta N_e}$ will be significantly less than $\bar{z}_{\mathrm{PSR}}$.

Table 5. Parameters of the $|z|$ distributions

Pulsar distribution	No. of pulsars	Vertical heights[A] (kpc) Mean $\bar{z}_{\mathrm{PSR}}$	Median $\bar{z}_{\mathrm{PSR}}$	Turbulence $\bar{z}_{\delta N_e}$[B]
All pulsars	83	0·251	0·190	0·204
$\|b\| < 5°$	47	0·137	0·073	0·087
$\|b\| \geqslant 5°$	36	0·400	0·372	0·541
$\|l\| < 60°$	45	0·236	0·169	0·172
$\|l\| > 60°$	38	0·269	0·255	0·329
$\|b\| < 5°$, $L < 3$ kpc	17	0·055	0·048	0·076
$\|b\| < 5°$, $L > 3$ kpc	29	0·190	0·143	0·141
$\|b\| < 5°$, $\|l\| < 60°$	31	0·165	0·095	0·119
$\|b\| < 5°$, $\|l\| > 60°$	15	0·089	0·063	0·144
$\|b\| \geqslant 5°$, $\|l\| < 60°$	12	0·390	0·363	0·381
$\|b\| \geqslant 5°$, $\|l\| > 60°$	21	0·393	0·360	0·556

[A] These averages omit 0833−45 and 1758−23, whose C_n^2 are extremely high relative to the remainder.
[B] Weighted average $|z|$ as defined by equation (4).

The values of $\bar{z}_{\delta N_e}$ for various subsets are listed in the last column of Table 5. It is evident from Table 5 that the values of $\bar{z}_{\delta N_e}$ are comparable with, or higher than, the $\bar{z}_{\mathrm{PSR}}$ values (the median values of $\bar{z}_{\mathrm{PSR}}$ are more reliable in small samples). This fact suggests that the scale height of the turbulence is comparable with, or probably greater than, the scale height of the pulsars; it is evidently true for both the high-latitude and low-latitude pulsars in general and for the subsets of low-latitude pulsars in particular. This conclusion does not agree with the results of Cordes *et al.* (1985) who, from a subset of 12 low-latitude pulsars ($|b| < 10°$), found $\bar{z}_{\delta N_e} \approx 0 \cdot 4\bar{z}_{\mathrm{PSR}}$ and for the high-latitude pulsars $\bar{z}_{\delta N_e} \approx \bar{z}_{\mathrm{PSR}}$. These authors used this result to postulate the presence of two scattering media, one with a scale height of <100 pc and the other with a scale height $\gtrsim 0 \cdot 5$ kpc. We have no evidence to support this suggestion; in fact, our results rather suggest the presence of one distribution of turbulence with scale height $> 0 \cdot 5$ kpc.

We have also computed the linear, power-law and exponential regressions of C_n^2 on $|z|$ for the various subsets of pulsars in Table 5. We found no relationships at better than the 80% confidence level; this supports the view that the scale height of the turbulence is greater than the median vertical height of any of the distributions in Table 5.

5. Discussion and Conclusions

We have reported new or revised measurements with the Culgoora circular array and the Parkes 64 m reflector of the scattering delay time τ on 33 pulsars. We have then combined these results with measurements of 52 other pulsars from the literature to compute the average turbulence levels C_n^2 along 85 paths through the Galaxy. Before discussing the implications of these measurements on the distribution of turbulence in the Galaxy we summarize our experimental conclusions.

(i) The pulse widening at 0·30 GHz is related to DM by a power law $\tau_{0.30} \propto \mathrm{DM}^{3.32}$ which applies over the whole observed range of $3 < \mathrm{DM} < 1140\ \mathrm{cm}^{-3}$ pc.

(ii) The level of turbulence is *apparently* related to the pulsar distance by an equation of the form $C_n^2 \propto \exp(0.46L)$ which applies quite generally to all directions in the Galaxy.

(iii) The best fit to the very scattered data implies a law of the form $C_n^2 \propto R^{-3}$.

(iv) Analysis of admittedly very scattered data for low-latitude pulsars ($|b| < 5°$) suggests an increase in C_n^2 by a factor of ~ 6.5 as the line of sight comes within $\sim 60°$ of the galactic centre. No such increase is seen for the high-latitude pulsars ($|b| \geqslant 5°$).

(v) The distribution of turbulence with vertical height as measured by $\bar{z}_{\delta N_e}$ of equation (4) is comparable with that of the pulsars.

We suggest that these findings are consistent with a distribution of scattering turbulence that peaks near the galactic centre and extends out to at least the solar circle in the plane of the Galaxy. It is not at all clear that we need to invoke the presence of a separate more extended scattering medium to explain the scattering of high-latitude pulsars and pulsars near the anti-centre, as has been suggested by Cordes *et al.* (1985). First, the fact that C_n^2 for the high-latitude pulsars does not show a galactocentric variation may be due to the restricted range of R (1·8 : 1) of this subset. Secondly, while the median C_n^2 varies by a factor of 6·8 between the low-latitude and high-latitude groups, most of this arises because of the apparent dependence of C_n^2 on heliocentric distance, which differs in the median by a factor of 4 between the groups. Our results would be consistent with one scattering medium having a scale height at least as great as that of the pulsars.

It seems that the magnitude of the fluctuations in electron density (δN_e) responsible for the scattering cannot be proportional to the average electron density (N_e). This is perhaps best shown by comparing the dependence of C_n^2 on galactocentric distance R with that given for N_e in the model of Lyne *et al.* (1985). These authors give a 2/1 variation in N_e in going from the galactic centre to the solar radius. Our regression equation $C_n^2 \propto R^{-3}$ yields a variation in C_n^2 of $\sim 1000/1$ over the same range of R in the galactic plane. Therefore, assuming $C_n^2 \propto \delta N_e^2$, we see that $\delta N_e/N_e$ increases by a factor of ~ 16 in going from the Sun to the galactic centre.

Our conclusion that there is a distribution of turbulence that peaks toward the galactic centre is consistent with the lack of interplanetary scintillators found by Rao and Ananthakrishnan (1985) at $|b| < 5°$ and $|l| < 30°$. There is also further evidence for unusually high scattering in this region of the Galaxy from VLBI measurements of the 408 MHz angular sizes of low-latitude sources by Dennison *et al.* (1984).

Finally, the apparent dependence of C_n^2 on pulsar distance is a well-established fact that argues strongly against the presence of homogeneous turbulence along a typical path through the Galaxy. The possible causes for this have been discussed in some detail by Cordes *et al.* (1985), who suggested that there may be at least two forms of non-uniformity that could give rise to an apparent increase of C_n^2 with distance: (i) strong clumping of the scattering turbulence so that the number of clumps encountered increases with the path-length; this of course may also help to explain the large variations in C_n^2 between pulsars at similar distances on nearby lines of sight; (ii) turbulence spectra that are more complex than power-law spectra so that different lines of sight effectively sample different wavenumber ranges.

There is now considerable evidence, from slow-intensity changes in pulsars (Sieber 1982; Slee *et al.* 1986) and slow, low-frequency variations in extragalactic sources (Slee 1984), that low-wavenumber enhancements of the turbulence spectrum probably exist. However, theoretical considerations (see e.g. Cordes *et al.* 1985) suggest that such a distortion in the wavenumber spectrum would, as well as making C_n^2 seem dependent on distance, make C_n^2 even more strongly dependent on observing frequency. The existing observations of scattering shown by several pulsars over an extended frequency range rather point to the existence of a simple power-law turbulence spectrum with an exponent near the Kolmogorov value of 11/3. Thus the simplest interpretation of the distance dependence for C_n^2 is the existence of a highly clumped (low filling factor) distribution of scattering irregularities along the various lines of sight.

Acknowledgments

We thank George A. Dulk for participating in the design of the Culgoora experiment and for carrying out some of the observations, R. N. Manchester and Lynette M. Newton for making available their Parkes observations, and Betty C. Siegman for assistance with the data analysis. We gratefully acknowledge the special time allocated to this project by the Computer Centre of the Physical Research Laboratory.

References

Cordes, J. M., Weisberg, J. M., and Boriakoff, V. (1985). *Astrophys. J.* **288**, 221.

Dennison, B., Thomas, M., Booth, R. S., Brown, R. L., Broderick, J. J., and Condon, J. J. (1984). *Astron. Astrophys.* **135**, 199.

Gullahorn, G. E., and Rankin, J. M. (1978). *Astron. J.* **83**, 1219.

Lyne, A. G., Manchester, R. N., and Taylor, J. H. (1985). *Mon. Not. R. Astron. Soc.* **213**, 613.

Manchester, R. N., D'Amico, N., and Tuohy, I. R. (1985). *Mon. Not. R. Astron. Soc.* **212**, 975.

Manchester, R. N., and Taylor, J. H. (1981). *Astron. J.* **86**, 1953.

Newton, L. M., Manchester, R. N., and Cooke, D. J. (1981). *Mon. Not. R. Astron. Soc.* **194**, 841.

Rankin, J. M., and Benson, J. M. (1981). *Astron. J.* **86**, 418.

Rao, A. P., and Ananthakrishnan, S. (1985). *Nature* **312**, 707.

Rickett, B. J. (1977). *Annu. Rev. Astron. Astrophys.* **15**, 479.

Roberts, J. A., and Ables, J. G. (1982). *Mon. Not. R. Astron. Soc.* **202**, 1119.
Sieber, W. (1982). *Astron. Astrophys.* **113**, 311.
Slee, O. B. (1984). *Mon. Not. R. Astron. Soc.* **209**, 215.
Slee, O. B., Alurkar, S. K., and Bobra, A. D. (1986). *Aust. J. Phys.* **39**, 103.
Slee, O. B., Dulk, G. A., and Otrupcek, R. E. (1980). *Proc. Astron. Soc. Aust.* **4**, 100.
Wolszczan, H., Hesse, K. H., and Sieber, W. (1974). *Astron. Astrophys.* **37**, 285.

Manuscript received 31 October 1985, accepted 23 January 1986